CRYSTAL GROWTH & DESIGN

ARTICLE

pubs.acs.org/crystal

A Case Study of Zn^{II}-bmb Meso-Helical Coordination Polymers upon the Spacer Angles and Lengths of Dicarboxylate Coligands

Chunying Xu, Qianqian Guo, Xianjuan Wang, Hongwei Hou,* and Yaoting Fan

Department of Chemistry, Zhengzhou University, Zhengzhou, Henan, 450052, People's Republic of China

Supporting Information

ABSTRACT: To systematically explore the influence of the spacer angles and lengths of dicarboxylate coligands on building Zn^{II}-bmb [1,4-bis(2-methylbenzimidazol-1-ylmethyl)benzene] meso-helical coordination polymers, we synthesized seven metal−organic frameworks $\{[Zn(bmb)_{0.5}(o\text{-}bdc)(H_2O)]\cdot 0.5(bmb)\cdot H_2O\}_n$ (**1**), $\{[Zn(bmb)(2,6\text{-}pydc)]\cdot 2H_2O\}_n$ (**2**), $[Zn(bmb)(m\text{-}bdc)]_n$ (**3**), $[Zn(bmb)_{0.5}(p\text{-}bdc)\cdot H_2O]_n$ (**4**), $[Zn(bmb)(fum)]_n$ (**5**), $\{[Zn(bmb)(suc)]\cdot 1.5H_2O\}_n$ (**6**), and $\{[Zn(bmb)(glu)]\cdot H_2O\}_n$ (**7**) (o-H_2bdc = 1,2-benzenedicarboxylic acid, 2,6-H_2pydc = 2,6-pyridinedicarboxylic acid, m-H_2bdc = 1,3-benzenedicarboxylic acid, p-H_2bdc = 1,4-benzenedicarboxylic acid, H_2fum = fumaric acid, H_2suc = succinic acid, and H_2glu = glutaric acid) through rationally varying the organic acid linkers. Structural analyses reveal that complexes **1**−**7** display diverse helical characters under the influence of dicarboxylates with different spacers. In complexes **1**, **2**, **3**, and **7**, the bmb ligands adopt *trans*-conformation bridging Zn^{II} ions to form rare meso-helices, which are further extended and decorated by different dicarboxylate coligands. Complex **4** exhibits a fascinating Borromean topology with three parallelly interlocked 6^3-hcb networks, in which p-bdc^{2-} and bmb with *trans*-conformation are linked by Zn^{II} ions to form a charming meso-helical chain. Complex **5** displays a 3-fold interpenetrated 3D diamonded network containing Zn^{II}/bmb/fum left- and right-handed helical microchannels. Complex **6** features unusual interweaved meso-helices constructed by *cis*- and *trans*-conformational bmb, which is the second example of tetra-flexural helix with four spiral shafts in one helical chain. In addition, the suc^{2-} anions further link Zn^{II}-bmb meso-helices to form a 3D framework. These results indicate that the spacers of dicarboxylate coligands and the conformations of bmb have important effects on the meso-helical characters and ultimate frameworks. Moreover, the investigation of photoluminescence properties of **1**−**7** reveals that the helical feature plays an important role in reducing photoluminescent intensities.

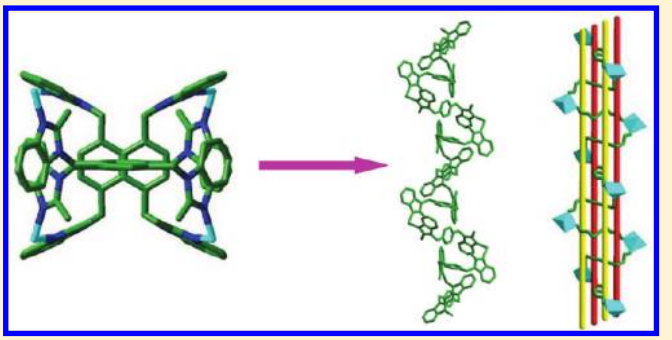

INTRODUCTION

Helical structures, the foundation of the genetic code, have attracted intense interest in coordination chemistry not only for their ubiquitous appearance in nature, a typical example being the DNA molecule, but also for their practical implications in multidisciplinary areas, such as optical devices, biomimetic chemistry, asymmetric catalysis chemistry, and structural biology.[1] Until now, many single-, double-, triple-, and even multiple-stranded helices as well as circular and cylindrical helices have been prepared and comprehensively discussed.[2] In contrast, the meso-helices are extremely infrequent,[3] although meso-helical motifs are common in nature, such as the tendrils of a variety of plants. The reason may be that it is quite difficult to control the formation of two or more flexures in single-stranded helix. Consequently, the rational design and construction of metal−organic frameworks (MOFs) with meso-helical character are still a long-term challenge. To get such meso-helices, the crucial step is to choose multifunctional organic ligands containing appropriate coordination sites linked by a proper spacer with specific positional orientation.[4] With this understanding, we select a semirigid N-heterocyclic ligand 1,4-bis(2-methylbenzimidazol-1-ylmethyl) benzene (bmb) with a rigid spacer of phenyl ring and two freely rotating methylbenzimidazol arms, which may generate two flexures and favor the formation of meso-helical motifs.[4a] In addition, the 2-position substituent methyl of benzimidazole ring can greatly enhance the donated electrons ability of the ligand,[5] which should be more likely to afford charming meso-helices.

It is well-known that dicarboxylate organic groups are excellent structural constructors.[6] Changes in the flexibility, length, spatial extended direction, and angle of the spacer can lead to remarkable classes of complexes bearing diverse architectures and functions.[7] In view of the development of synthetic strategy,[8] it will be valuable to introduce the dicarboxylates with different spacers into the meso-helices synthetic process based on N-donor ligand bmb, which can result in greater tunability of the meso-helical features and build much more complicated and fascinating MOFs. Moreover, a systematic investigation about the influence of the spacer angles and lengths of dicarboxylate

Received: January 14, 2011
Revised: March 15, 2011
Published: March 25, 2011

dx.doi.org/10.1021/cg200052t | *Cryst. Growth Des.* 2011, 11, 1869–1879

Table 1. Crystal Data and Structure Refinement for Complexes 1−7[a]

complex no.	1	2	3	4	5	6	7
formula	$C_{32}H_{30}N_4O_6Zn$	$C_{31}H_{29}N_5O_6Zn$	$C_{32}H_{26}N_4O_4Zn$	$C_{20}H_{17}N_2O_5Zn$	$C_{28}H_{24}N_4O_4Zn$	$C_{28}H_{29}N_4O_{5.5}Zn$	$C_{29}H_{30}N_4O_5Zn$
formula mass	632.01	633.00	595.98	430.77	545.92	574.96	579.98
temperature (K)	293(2)	293(2)	293(2)	293(2)	293(2)	293(2)	293(2)
wavelength (Å)	0.71073	0.71073	0.71073	0.71073	0.71073	0.71073	0.71073
crystal system	triclinic	monoclinic	monoclinic	triclinic	monoclinic	monoclinic	monoclinic
space group	$P\bar{1}$	$C2/c$	$C2/c$	$P\bar{1}$	$C2/c$	$C2/c$	$C2/c$
a (Å)	11.019(2)	18.611(4)	18.250(4)	9.5601(19)	20.821(4)	29.464(6)	8.6678(17)
b (Å)	12.405(3)	11.410(2)	17.648(3)	10.616(2)	10.684(2)	10.887(2)	19.885(4)
c (Å)	12.645(3)	15.455(3)	19.003(4)	10.931(2)	15.656(3)	21.025(4)	15.938(3)
α (°)	66.04(3)	90.00	90.00	108.47(3)	90.00	90.00	90.00
β (°)	75.42(3)	114.84(3)	117.73(3)	110.01(3)	127.10(3)	129.66(3)	91.66(3)
γ (°)	69.48(3)	90.00	90.00	103.74(3)	90.00	90.00	90.00
V (Å^3)	1467.2(6)	2978.3(10)	5417.5(24)	911.1(5)	2777.7(14)	5192.1(28)	2745.9(9)
Z	2	4	8	2	4	4	4
D_{calcd} (g cm^{-3})	1.426	1.403	1.461	1.570	1.305	1.463	1.403
μ (mm^{-1})	0.889	0.876	0.953	1.383	0.922	0.995	0.940
F(000)	652	1296	2463	442	1128	2368	1208
θ (°)	2.08−25.00	2.30−29.14	1.71−24.99	2.19−29.13	2.27−29.15	2.52−25.00	2.41− 25.00
data/restraints/parameters	5081/3/393	3980/0/197	4664/10/392	4827/0/259	3739/0/169	4547/0/354	2348/0/187
GOF	1.070	1.083	1.060	1.062	1.041	1.069	1.055
R_1 [$I > 2\sigma(I)$]	0.0646	0.0509	0.0653	0.0552	0.0484	0.0410	0.0870
wR_2 [$I > 2\sigma(I)$][b]	0.1480	0.1422	0.1645	0.0986	0.1369	0.1102	0.2023

[a] $R_1 = ||F_o| - |F_c||/|F_o|$. [b] $wR_2 = [w(F_o^2 - F_c^2)^2/w(F_o^2)^2]^{1/2}$.

coligands on the assembly processes of MOFs with meso-helical character is also valuable.

On the basis of the above considerations, by introducing a series of dicarboxylate coligands with different spacer angles and lengths into the Zn^{II}-bmb synthesis system, fascinating meso-helical coordination polymers, namely, $\{[Zn(bmb)_{0.5}(o\text{-}bdc)(H_2O)]\cdot 0.5(bmb)\cdot H_2O\}_n$ (**1**), $\{[Zn(bmb)(2,6\text{-}pydc)]\cdot 2H_2O\}_n$ (**2**), $[Zn(bmb)(m\text{-}bdc)]_n$ (**3**), $[Zn(bmb)_{0.5}(p\text{-}bdc)\cdot H_2O]_n$ (**4**), $[Zn(bmb)(fum)]_n$ (**5**), $\{[Zn(bmb)(suc)]\cdot 1.5H_2O\}_n$ (**6**), and $\{[Zn(bmb)(glu)]\cdot H_2O\}_n$ (**7**) were synthesized under similar hydrothermal conditions. The meso-helical structural analysis, along with a systematic investigation about the influence of the spacer angles and lengths of dicarboxylate coligands on framework characters, is represented and discussed. In addition, the thermal stabilities and photoluminescence properties of **1**−**7** in the solid state have also been investigated.

EXPERIMENTAL SECTION

Materials and Physical Measurements. All reagents and solvents were commercially available except for bmb, which was synthesized according to the literature.[9] The Fourier transform infrared spectra were recorded from KBr pellets in the range of 400−4000 cm^{-1} on a Bruker Tensor 27 spectrophotometer. Elemental analyses (C, H, and N) were carried out on a FLASH EA 1112 elemental analyzer. PXRD patterns were recorded using Cu Kα1 radiation on a PANalytical X'Pert PRO diffractometer. Thermal analyses were performed on a Netzsch STA 449C thermal analyzer from room temperature at a heating rate of 10 °C min^{-1} in air. The luminescence spectra for the powdered solid samples were measured at room temperature on a Hitachi F-4500 Fluorescence Spectrophotometer. The excitation slit and the emission slit were 2.5 nm.

Synthesis of $\{[Zn(bmb)_{0.5}(o\text{-}bdc)(H_2O)]\cdot 0.5(bmb)\cdot H_2O\}_n$ (***1***). A mixture of $Zn(Ac)_2\cdot 2H_2O$ (43.9 mg, 0.2 mmol), bmb (36.6 mg, 0.1 mmol), o-H_2bdc (33.2 mg, 0.2 mmol), and NaOH (8.0 mg, 0.2 mmol) in 10 mL of distilled H_2O was sealed in a 25 mL Teflon-lined stainless steel container and heated at 160 °C for 4 days. After the mixture was cooled to room temperature at a rate of 5 °C/h, colorless block crystals of **1** were obtained with a yield of 56% (based on Zn). Anal. calcd for $C_{32}H_{30}N_4O_6Zn$ (%): C, 60.81; H, 4.78; N, 8.86. Found: C, 61.09; H, 4.50; N, 9.05. IR (KBr, cm^{-1}): 3440 (s), 3053 (w), 2361 (s), 2337 (s), 1616 (s), 1514 (w), 1458 (m), 1371 (s), 1290 (w), 1143 (s), 1014 (m), 986 (w), 859 (m), 826 (m), 750 (s), 672 (m), 618 (m).

$\{[Zn(bmb)(2,6\text{-}pydc)]\cdot 2H_2O\}_n$ (***2***). The same synthetic method as that for **1** was used except that o-H_2bdc was replaced by 2,6-H_2pydc (33.4 mg, 0.2 mmol). Yield, 60% (based on Zn). Anal. calcd for $C_{31}H_{29}N_5O_6Zn$ (%): C, 58.82; H, 4.62; N, 11.06. Found: C, 58.57; H, 4.46; N, 10.82. IR (KBr, cm^{-1}): 3467 (s), 2984 (w), 1639 (s), 1610 (m), 1592 (w), 1506 (w), 1491 (m), 1460 (s), 1367 (s), 1291 (m), 1274 (m), 1182 (m), 1079 (s), 1016 (m), 906 (m), 860 (m), 761 (s), 747 (m), 729 (w), 675 (m), 617 (m), 470 (w).

$[Zn(bmb)(1,3\text{-}bdc)]_n$ (***3***). The same synthetic method as that for **1** was used except that o-H_2bdc was replaced by m-H_2bdc (33.2 mg, 0.2 mmol). Yield, 18% (based on Zn). Anal. calcd for $C_{32}H_{26}N_4O_4Zn$ (%): C, 64.49; H, 4.39; N, 9.40. Found: C, 64.62; H, 4.52; N, 9.24. IR (KBr, cm^{-1}): 3065 (m), 1623 (s), 1592 (s), 1503 (m), 1479 (m), 1459 (m), 1376 (m), 1361 (m), 1337 (s), 1292 (m), 1268 (m), 1227 (w), 1167 (s), 1073 (m), 1014 (m), 987 (m), 859 (m), 715 (s), 615 (m), 465 (m).

$[Zn(bmb)_{0.5}(p\text{-}bdc)\cdot H_2O]_n$ (***4***). The same synthetic method as that for **1** was used except that o-H_2bdc was replaced by p-H_2bdc (33.2 mg, 0.2 mmol). Yield, 48% (based on Zn). Anal. calcd for $C_{20}H_{17}N_2O_5Zn$ (%): C, 55.76; H, 3.98; N, 6.50. Found: C, 55.81; H, 4.12; N, 6.34. IR (KBr, cm^{-1}): 3435 (s), 2925 (w), 2360 (w), 1613 (s), 1584 (s), 1516 (s), 1499 (s), 1459 (m), 1415 (w), 1384 (m), 1350 (s), 1294 (m), 1145 (m), 1016 (s), 878 (m), 820 (s), 749 (s), 676 (w), 588 (m).

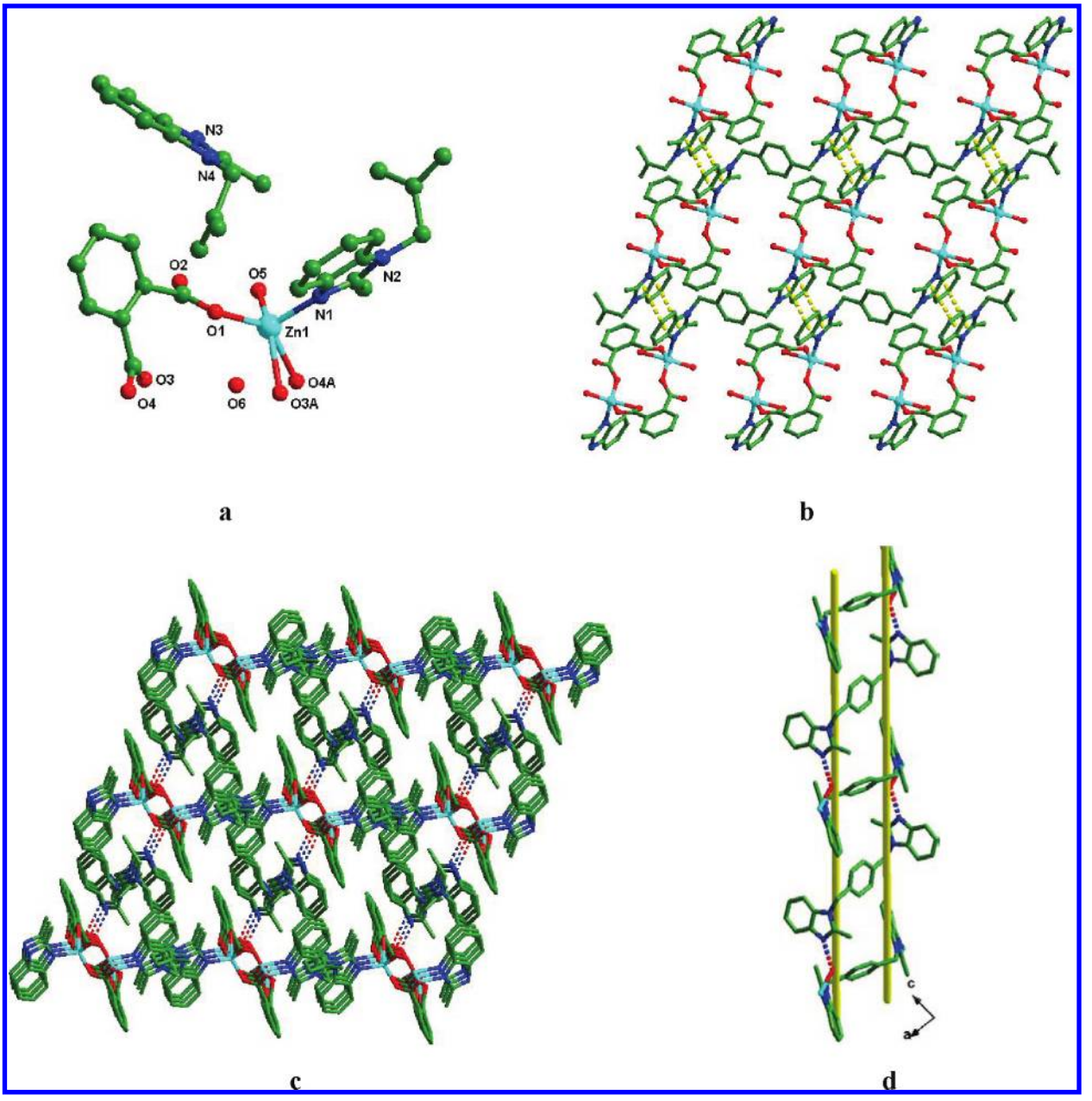

Figure 1. (a) Asymmetric unit of **1** with hydrogen atoms omitted for clarity. (b) A 2D sheet formed through $\pi-\pi$ stacking interactions. (c) A 3D supramolecular lattice of **1** directed by O−H···N hydrogen-bonding and $\pi-\pi$ stacking interactions. (d) A 1D supramolecular meso-helical chain.

[Zn(bmb)(fum)]$_n$ (***5***). The same synthetic method as that for **1** was used except that o-H_2bdc was replaced by H_2fum (23.2 mg, 0.2 mmol). Yield, 62% (based on Zn). Anal. calcd for $C_{28}H_{24}N_4O_4Zn$ (%): C, 61.60; H, 4.43; N, 10.26. Found: C, 61.49; H, 4.50; N, 10.33. IR (KBr, cm^{-1}): 3058 (w), 2360 (m), 1608 (s), 1504 (m), 1477 (m), 1458 (s), 1416 (m), 1341 (s), 1290 (s), 1224 (w), 1166 (m), 1129 (w), 1015 (m), 985 (s), 922 (w), 872 (w), 858 (m), 798 (m), 755 (s), 688 (m), 670 (m), 615 (s), 581 (m), 483 (m).

{[Zn(bmb)(suc)]·1.5H_2O}$_n$ (***6***). The same synthetic method as that for **1** was used except that o-H_2bdc was replaced by H_2suc (23.6 mg, 0.2 mmol). Yield, 57% (based on Zn). Anal. calcd for $C_{28}H_{29}N_4O_{5.5}Zn$ (%): C, 58.49; H, 5.08; N, 9.74. Found: C, 58.73; H, 5.12; N, 9.94. IR (KBr, cm^{-1}): 3425 (s), 2925 (w), 1625 (s), 1578 (m), 1513 (s), 1475 (w), 1459 (s), 1419 (s), 1384 (s), 1293 (w), 1270 (s), 1228 (w), 1184 (w), 1162 (w), 1016 (m), 987 (m), 871 (s), 703 (w), 616 (m), 553 (w), 434 (w).

{[Zn(bmb)(glu)]·H_2O}$_n$ (***7***). The same synthetic method as that for **1** was used except that o-H_2bdc was replaced by H_2glu (26.4 mg, 0.2 mmol). Yield, 48% (based on Zn). Anal. calcd for $C_{29}H_{30}N_4O_5Zn$ (%): C, 60.06; H, 5.21; N, 9.66. Found: C, 60.15; H, 5.37; N, 9.74. IR (KBr, cm^{-1}): 3435 (s), 2968 (w), 2360 (m), 2342 (m), 1590 (s), 1509 (w), 1481 (w), 1459 (m), 1443 (w), 1415 (s), 1292 (w), 1229 (m), 1164 (w), 1014 (w), 993 (m), 927 (m), 876 (m), 744 (s), 669 (m), 614 (w), 552 (w), 476 (w).

Crystal Data Collection and Refinement. The data of the seven complexes were collected on a Rigaku Saturn 724 CCD diffractomer (Mo Kα, λ = 0.71073 Å) at a temperature of 20 ± 1 °C. Absorption corrections were applied by using a multiscan program. The data were corrected for Lorentz and polarization effects. The structures were solved by direct methods and refined with a full-matrix least-squares technique based on F^2 with the SHELXL-97 crystallographic software package.[10]

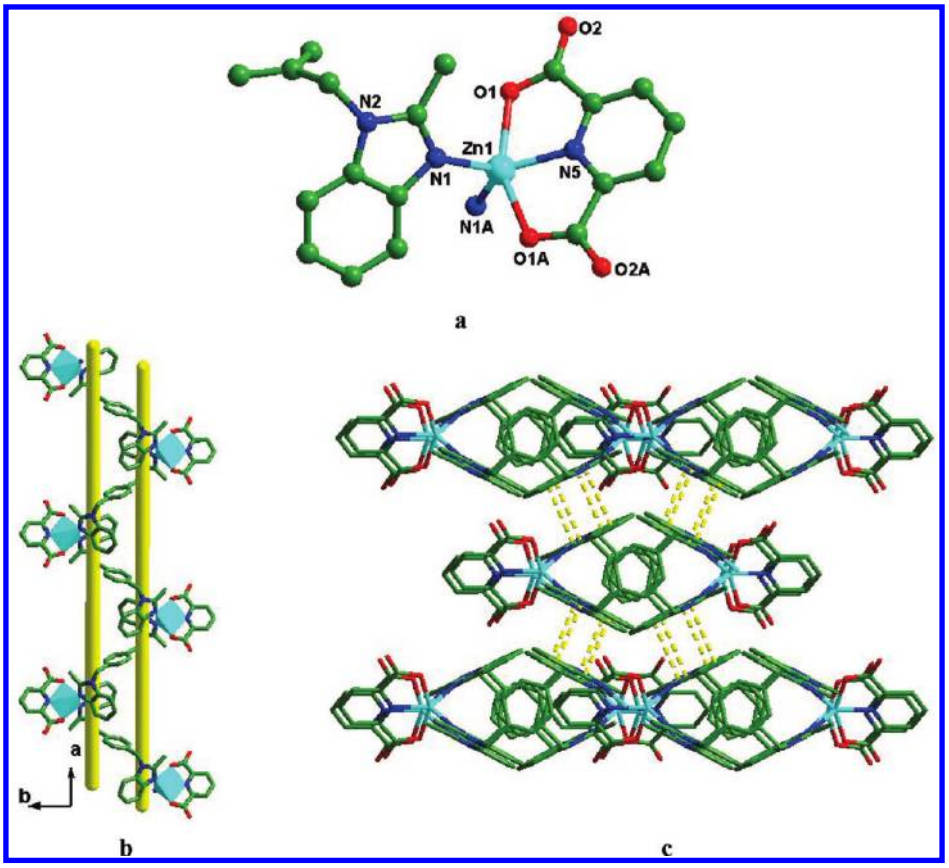

Figure 2. (a) Coordination environment of Zn^{II} ion in **2** with hydrogen atoms and free water molecules omitted for clarity. (b) View of the 1D meso-helical chain of **2**. (c) The discrete meso-helical chains are interconnected to form 3D supramolecular by $\pi-\pi$ stacking interactions.

The hydrogen atoms of carbon were placed at calculated positions and refined as riding atoms with isotropic displacement parameters. The hydrogen atoms of part of water were located from Fourier difference maps with suitable restraint, and part of those could not be located in the difference map. In complex **3**, distances restraints (SADI and DFIX) were applied in the unreasonable benzene ring (C31−C32−C33−C32A−C31A−C34) and disordered carboxylic groups (O3−C30−O4 and O3′−C30′−O4). Higher than expected R1 value (0.0870) of **7** is attributed to weak diffraction resulting from poor quality of the crystal itself. Crystallographic crystal data and structure processing parameters for **1**−**7** are summarized in Table 1. Selected bond lengths and bond angles of **1**−**7** are listed in Table S1 in the Supporting Information.

RESULTS AND DISCUSSION

Design and Synthesis of Complexes. The conformation and flexibility of ligands are considered to be the key factors for the formation of meso-helical features. Semirigid ligand 1,4-bis-(2-methylbenzimidazol-1-ylmethyl) benzene (bmb) contains a rigid spacer of phenyl ring and two freely rotating methylbenzimidazol arms. The optimized energy calculation of bmb (−719833.158 kcal/mol for *cis*-conformation and −719833.4805 kcal/mol for *trans*-conformation) indicates that it can show stable *cis*- and *trans*-conformations, and the two conformations can transform to each other to suit the coordinated environment of the metal centers. The reason may be that the flexible −CH_2− makes the two methylbenzimidazol groups significantly deviate from co-planarity with a potential tendency to generate various *cis*- and *trans*-conformations when bmb coordinates with metal centers.[11] Such "skewing" of coordination sites and various conformations in bmb should favor the formation of meso-helical motifs. In addition, the 2-position substituent methyl can enhance the donated electrons ability of benzimidazole ring, and the bmb ligand exhibits strong collaborative coordination ability with organic carboxylate ligands. Moreover, it has been demonstrated that the structural diversities of the complexes are undoubtedly related to the secondary ligand-directed inclusion.[12] So, the introduction of dicarboxylate coligands may effectively adjust the meso-helical features and build much more complicated and fascinating MOFs.

In complex **1**, we select o-H_2bdc with a rigid spacer and an angle of 60° between the two carboxylic groups as a coligand. Two o-H_2bdc chelate two Zn^{II} ions to form a dual-core unit and the free and coordinated bmb ligands with *trans*-conformation link Zn^{II} ions to afford a rare meso-helical through coordination bond and hydrogen-bonding interactions. By introducing 2,6-H_2pydc with a larger angle of 120°, a distinct meso-helical chain **2** decorated with 2,6-$pydc^{2-}$ at both sides is constructed. Investigation of the overall structures of **1** and **2**, the chelating characteristic of the dicarboxylate ligands, plays an important role in the formation of 1D complexes. In **3**, m-H_2bdc links the Zn^{II}-bmb meso-helical chain leading to a 2D puckered net. Increasing the angle between two carboxylic groups to 180° (p-H_2bdc), a fascinating Borromean topology of **4** containing three parallelly interlocked 6^3-hcb networks is obtained, in which p-bdc^{2-} and bmb with *trans*-conformation are linked by Zn^{II} ions to generate a charming meso-helical chain. Obviously, with the increasing angle between two carboxylic groups, higher dimensionality

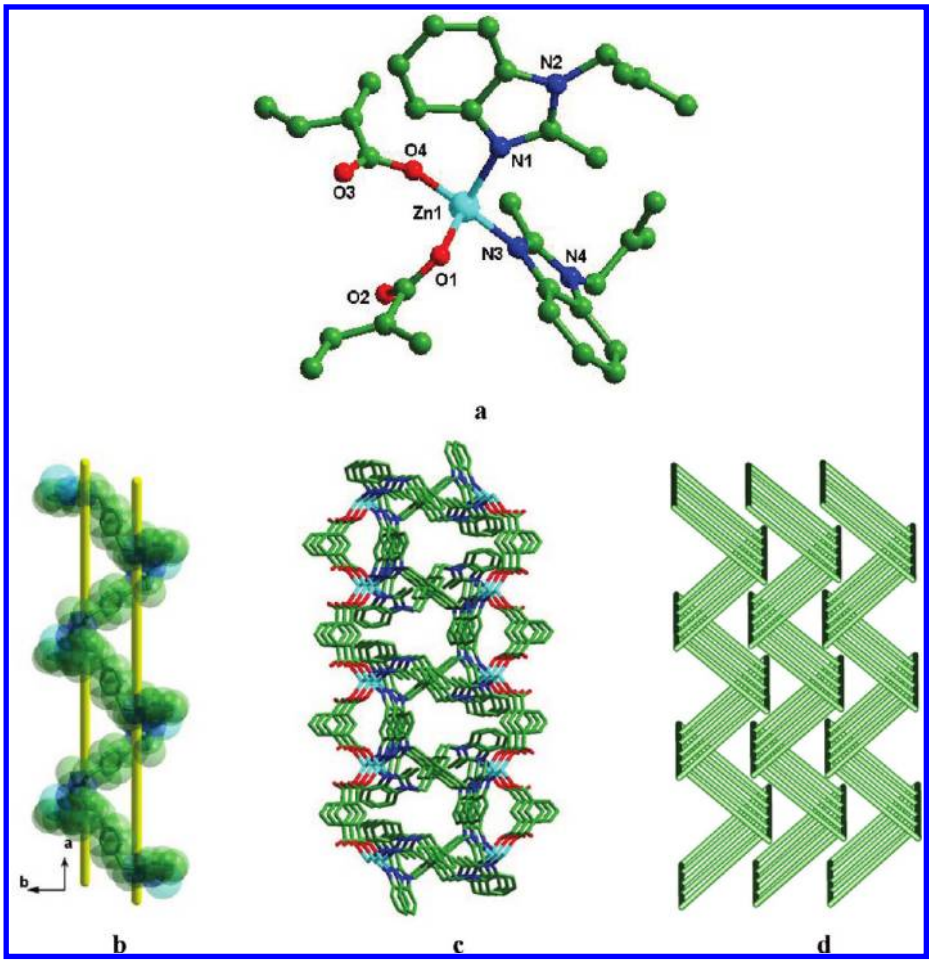

Figure 3. (a) Coordination environment of Zn^{II} ion in **3** with hydrogen atoms omitted for clarity. (b) The bmb ligands with *trans*-conformation link the adjoining Zn^{II} ions into a 1D meso-helical chain. (c) The Zn^{II}-bmb meso-helices are extended to a 2D layer structure by the bridging of m-bdc^{2-} anions. (d) The puckered (4, 4) net of **3**.

complexes are easy to form. When H_2fum with an extended rigid −CH═CH− spacer instead of benzene ring is introduced into the synthetic procedure, a 3-fold interpenetrated 3D diamonded network structure **5** with Zn^{II}/bmb/fum left- and right-handed helical microchannels is obtained. The flexible suc^{2-} linking Zn^{II}-bmb meso-helical chain produces a 3D framework **6**. Interestingly, the suc^{2-} anions coordinate with Zn^{II} ions to form a left-hand helix, and at the same time, the *cis*- and *trans*-conformational bmb ligands are linked by Zn^{II} ions alternately to form unusual interweaved meso-helices, which is the second example of tetra-flexural helix with four spiral shafts in one helical chain. The formations of 3D frameworks **5** and **6** indicate that the dicarboxylate coligands with small steric hindrance favor the generation of higher dimensional products. Extending the spacer length into $-(CH_2)_3-$, the *trans*-conformational bmb ligands form a meso-helix by coordinating with Zn^{II} ions, and the helices are further linked by glu^{2-} to produce a 2D puckered net **7**, which may be due to that the high flexibility of glu^{2-} leads to the slightly chelating characteristic.

It can be observed that **1**, **2**, **3**, and **7** display different aspects of meso-helices constructed by bmb and Zn^{II} ions, which are probably due to the slight regulation of different dicarboxylate coligands; in **4**, p-bdc^{2-} takes part in the formation of the meso-helix; in **6**, the left-handed helix formed by suc^{2-} and Zn^{II} ions induces the fascinating interweaved meso-helices; however, fum^{2-}, Zn^{II} ions, and bmb together form the single-stranded helix instead of meso-helix as a result of the formation of 3-fold diamonded interpenetrated network in **5**. The results confirm that the semirigid ligand bmb is an excellent meso-helical constructor. Subtle spacer variation of dicarboxylate coligands has a significant influence on the formation of meso-helical features and overall framework.

Crystal Structure of $\{[Zn(bmb)_{0.5}(o\text{-}bdc)(H_2O)]\cdot 0.5(bmb)\cdot H_2O\}_n$ (***1***). Single-crystal X-ray diffraction analysis shows that the asymmetric unit of **1** consists of one Zn^{II} ion, one o-bdc^{2-} anion, half coordinated bmb, one coordinated water molecule, half free bmb, and one guest water molecule (Figure 1a). The Zn^{II} ion is five-coordinated in a distorted square-pyramidal geometry, defined by O1, O3A, and O4A from two symmetry-related o-bdc^{2-} anions and O5 from the coordinated water molecule in the base positions, and one N1 from one bmb ligand in the axial site. The Zn−O bond lengths range from 1.972(3) to 2.240(5) Å, and the Zn−N bond length is 2.017(3) Å. The two carboxylic groups of each o-bdc^{2-} anion adopt different coordination modes: one with μ_2-η^1:η^1-bidentate bridging mode and the other one with μ_1-η^1:η^0-mode. Two o-bdc^{2-} anions with a small angle of 60° between two carboxylic groups give rise to a closed loop by coordinating to two Zn^{II} ions

dx.doi.org/10.1021/cg200052t |*Cryst. Growth Des.* 2011, 11, 1869–1879

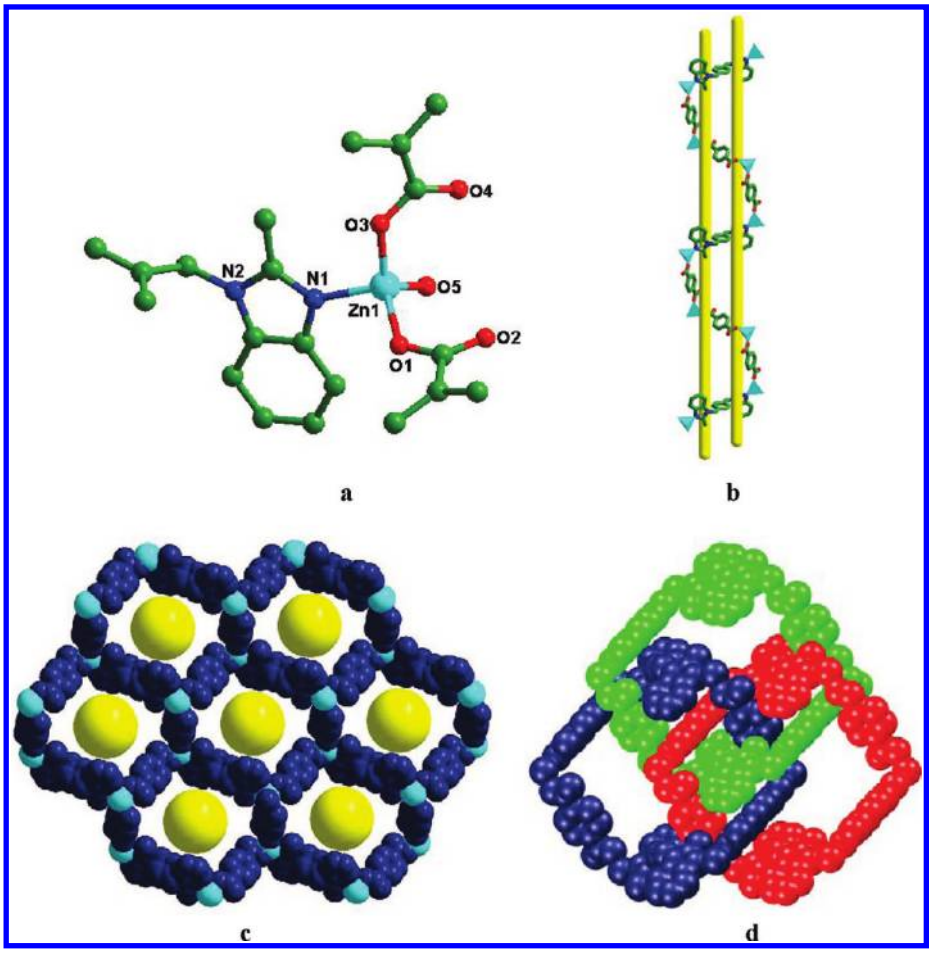

Figure 4. (a) Coordination environment of Zn^{II} ion in **4** with hydrogen atoms and free water molecules omitted for clarity. (b) View of the meso-helical chain of Zn^{II}/bmb/p-bdc. (c) The 2D (6, 3) hcb network based on hexagonal ring, which involves four p-bd^{2-} anions, two bmb ligands, and six Zn^{II} ions. (d) Space-filling representation of a Borromean links in the honeycomb-like sheets.

resulting in a $Zn_2(o\text{-}bdc)_2$ metallocyclic motif. The $Zn_2(o\text{-}bdc)_2$ units are linked by bmb leading to a 1D zigzag chain and further form a 2D sheet by $\pi-\pi$ stacking interactions of benzimidazole rings [3.6769(18) Å] (Figure 1b). The 2D sheets are interlinked to produce a 3D dimensional supramolecular framework (Figure 1c) through O−H···N hydrogen-bonding interactions [2.6617(53) Å]. In addition, in **1**, both the free and the coordinated bmb adopt *trans*-conformation with different $N_{donor}\cdots N-C_{sp3}\cdots C_{sp3}$ torsion angles of 100.353 and 90.928°, respectively. Under the coordination bond and hydrogen bond, two types of bmb are linked together by ZnO units, affording an extraordinary *meso*-helical chain (Figure 1d) with Zn···Zn distances of 14.19 and 19.13 Å, respectively.

Crystal Structure of $\{[Zn(bmb)(2,6\text{-}pydc)]\cdot 2H_2O\}_n$ (**2**). Single-crystal X-ray structural analysis reveals that **2** is a 1D meso-helical chain with a charming packing motif. As shown in Figure 2a, the Zn^{II} ion adopts a distorted trigonal-dipyramidal geometry via coordinating with three nitrogen atoms from one 2,6-$pydc^{2-}$ anion (N5) and two symmetry-related bmb (N1, N1A) in the equatorial plane as well as two oxygen atoms (O1, O1A) from different carboxylic groups of one 2,6-$pydc^{2-}$ anion at the axial site. The Zn−N bond lengths vary from 2.0030(2) to 2.0049(18) Å, while the Zn−O bond lengths are 2.2214(17) Å, which are in the normal range.[13] In **2**, bmb also adopts the *trans*-conformation with a $N_{donor}\cdots N-C_{sp3}\cdots C_{sp3}$ torsion angle of 80.221°, which displays two flexures with opposite direction. The bmb bridging neighboring Zn^{II} ions afford a fascinating *meso*-helical chain with left- and right-handed helical loops in one single strand along the *c*-axis. The helical pitch is 18.535 Å corresponding to the length of the *a*-axis, and the Zn···Zn separation across the bmb bridge is 13.680 Å. Although the angle between two carboxylic groups increases to 120°, the 2,6-$pydc^{2-}$ anions still show tridentate chelating mode due to the existence of the N-donor atom between two carboxylic groups. The 1D Zn-bmb meso-helical motif is decorated with 2,6-$pydc^{2-}$ anions at both sides in an approximately parallel fashion (Figure 2b). Moreover, the discrete meso-helical chains are interconnected to produce a tempting 3D supramolecular framework by $\pi-\pi$ stacking interactions [3.5440(6) Å] of benzimidazole rings (Figure 2c) that further stabilize the crystal structure.

Crystal Structure of $[Zn(bmb)(m\text{-}bdc)]_n$ (**3**). As depicted in Figure 3a, the coordination environment around the Zn^{II} center is best portrayed as a slightly distorted $[ZnN_2O_2]$ tetrahedral geometry, ligated by two oxygen atoms (O1, O4) from two different m-bdc^{2-} anions and two nitrogen atoms (N1, N3) from two distinct bmb. The bond lengths are Zn(1)−O(1) = 1.971(3), Zn(1)−O(4) = 1.894(4), Zn(1)−N(1) = 2.041(4), and Zn(1)−N(3) = 2.031(4) Å, respectively. There are two kinds of independent bmb, both of which exhibit *trans*-conformation with smaller $N_{donor}\cdots N-C_{sp3}\cdots C_{sp3}$ torsion angles of

dx.doi.org/10.1021/cg200052t |*Cryst. Growth Des.* 2011, 11, 1869–1879

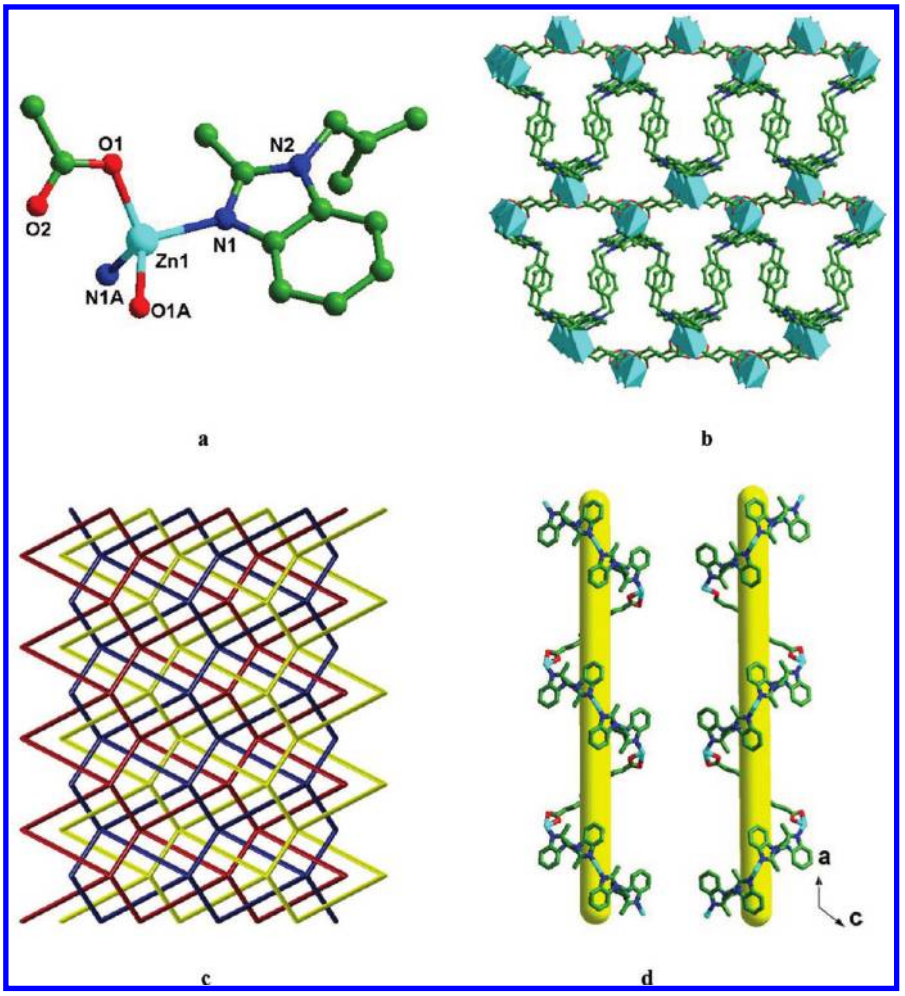

Figure 5. (a) Coordination environment of Zn^{II} ion in **5** with hydrogen atoms omitted for clarity. (b) View of the 3D puckered grid accomplished by connecting four linear ligands (two bmb and two fum^{2-}) to four different Zn^{II} ions. (c) The 3-fold interpenetrating dia topology. (d) The Zn^{II}/bmb/fum left- and right-handed helical chains along the *c*-axis.

78.648 and 76.685° than those of complexes **1** and **2**. The two types of bmb act as bidentate mode to bridge two adjacent Zn^{II} ions alternately resulting in a meso-helical motif (Figure 3b). The Zn···Zn separations across the bmb bridges are 14.278 and 14.316 Å, respectively. Hinging at metal ions, the pitch of the meso-helix is 19.272 Å, corresponding to the length of *c*-axis. By introducing the bis-monodentate m-bdc^{2-} with an angle of 120° between two carboxylic groups, the Zn-bmb meso-helices are further extended to a 2D layer (Figure 3c), and the Zn···Zn distance across m-bdc^{2-} is 8.7022(21) Å. Topology analysis indicates that the 2D layer is a puckered (4, 4) net (Figure 3d) with regard to Zn^{II} ion as a node.

Crystal Structure of $[Zn(bmb)_{0.5}(p\text{-}bdc)\cdot H_2O]_n$ (**4**). Single-crystal X-ray diffraction analysis shows that **4** is a enchanting 2D Borromean layerlike structure. The Zn^{II} center displays a distorted tetrahedral geometry (Figure 4a), which is provided by two oxygen atoms (O1, O3) from two distinct p-bdc^{2-} anions, one oxygen atom (O5) from one water molecule, and one nitrogen atom (N1) from bmb. The bond lengths of Zn−O and Zn−N are similar to those in other zinc-coordinated complexes.[13] In **4**, bmb adopts *trans*-conformation with a $N_{donor}\cdot\cdot\cdot N{-}C_{sp3}\cdot\cdot\cdot C_{sp3}$ torsion angle of 96.700°, and the two methylbenzimidazol arms bend in opposite directions to bridge two adjacent Zn^{II} ions with a distance of 16.684 Å. The linear type p-bdc^{2-} anion adopts simple bis-monodentate mode bridging two adjacent Zn^{II} ions. Every three p-bdc^{2-} anions are linked by four Zn^{II} ions to form a "Z" shape with a $Zn^{II}\cdots Zn^{II}\cdots Zn^{II}\cdots Zn^{II}$ torsion angle of 180°. Such "Z" shapes are bridged by *trans*-conformational bmb to build a meso-helical chain (Figure 4b). The repeating pitch of the helix with four Zn^{II} ions, one bmb, and three p-bdc^{2-} spans a long distance of 28.680 Å corresponding to three times of the length of *a*-axis.

On the other hand, every two bmb and four p-bdc^{2-} are connected by six Zn^{II} ions to construct a chair conformational $[Zn(bmb)_2(p\text{-}bdc)_4]$ hexagonal ring. The ring diameters, defined as the distance between two symmetry-related opposing Zn^{II} ions, range from 20.2746(45) to 24.1868(48) Å. Adjacent rings share edges and vertices to form a 2D (6, 3) undulated honeycomb (hcb) net, as shown in Figure 4c. Further structural analysis reveals that there are three identical hcb networks entangled in one layer. Any two of the three parallelly interlocked networks are actually noncatenated and noninterpenetrated, but appearance of the third network causes an inseparable interweaving, which is the characteristic of Borromean topology.[14] From Figure 4d, we can easily realize this point by observing that the red ring is located above the blue one, the green net above the

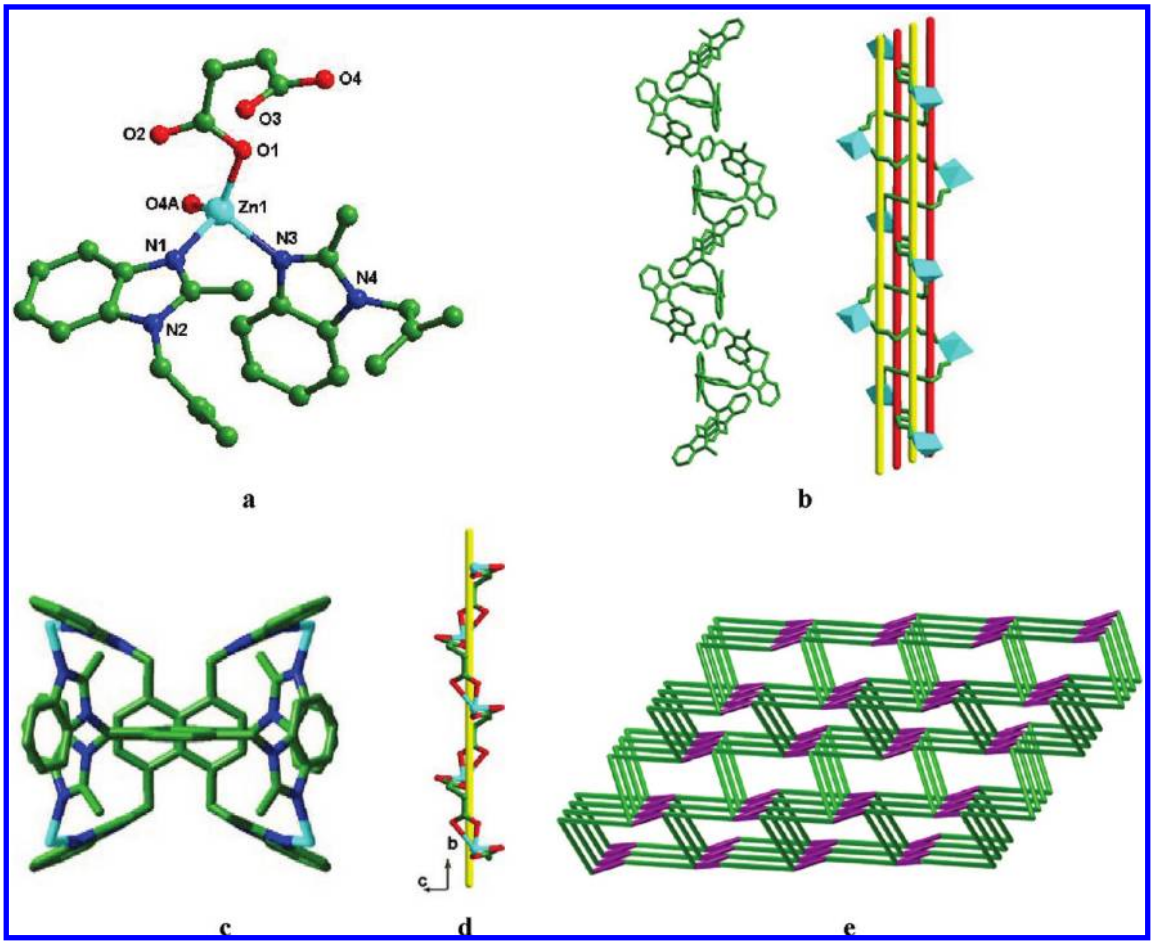

Figure 6. (a) Coordination environment of Zn^{II} ion in **6** with hydrogen and free water molecules atoms omitted for clarity. (b) View of the single-stranded meso-helix with a tetraflexural nod. (c) The projection of tetraflexural helical chain on the *ab* plane looks like a pair of swallows standing face to face. (d) The suc^{2-} anions coordinate with Zn^{II} ions to form a left-hand helix. (e) Schematic view of the 6^6 topology of **6**.

red one, but the blue ring lies above the green one, and no individual ring is interlocked to another without the help of the third one. The formation of this puzzling entanglement can be attributed to the large hcb voids and the corrugation of the single sheet, which are believed as the critical requirement for the formation of Borromean links. In addition, adjacent Borromean lays are interconnected by O−H···O [2.625(5) and 2.629(3) Å] hydrogen-bonding interactions that further stabilize the crystal structure.

*Crystal Structure of [Zn(bmb)(fum)]$_n$ (**5**).* The structure of **5** contains a tetrahedral Zn^{II} atom (Figure 5a), which is coordinated by two symmetry-related fum^{2-} anions and two symmetry-related bmb ligands with the Zn−O and Zn−N bond lengths of 1.977(3) and 2.052(3) Å, respectively. The bmb adopts *trans*-conformation with a $N_{donor}\cdots N-C_{sp3}\cdots C_{sp3}$ torsion angle of 96.653° to connect two adjacent Zn^{II} ions. Each deprotonated carboxylic group of fum^{2-} acts as monodentate mode to coordinate with adjacent Zn^{II} ions. The extension of the structure into a 3D network is accomplished by connecting four linear ligands (two bmb and two fum^{2-}) to four different Zn^{II} ions. As can be seen in Figure 5b, the Zn···Zn distances across bmb and m-bdc^{2-} are 14.679 and 8.800 Å, respectively. A further analysis indicates that it is a typical diamondoid framework containing large cages, which are elongated significantly in one direction, and exhibit maximum dimensions (corresponding to the longest intracage Zn···Zn distances of 32.0 Å × 25.049 Å × 20.821 Å). The potential voids are filled via mutual interpenetration of the other two independent equivalent diamondoid frameworks in a normal mode, giving rise to a 3-fold interpenetrating dia array (Figure 5c).

In contrast of above complexes, it is notable that instead of the meso-helix, the left- and right-handed helices (Figure 5d) with large quadrilateral microchannels (Zn^{II}−bmb−Zn^{II}−bmb−Zn^{II}−fum−Zn^{II}−fum−Zn^{II})$_n$ are constructed. Both of the helical pitches are 20.821(4) Å corresponding to the length of *a*-axis. The reason may be that the formation of the interpenetrating structure needs large cages.

*Crystal Structure of {[Zn(bmb)(suc)]·1.5H_2O}$_n$ (**6**).* As illustrated in Figure 6a, the tetrahedral Zn^{II} ion is coordinated by two symmetry-related oxygen atoms (O1, O4) from two suc^{2-} anions and two nitrogen atoms (N1, N3) from two distinct bmb with the average Zn−O and Zn−N bond distances of 1.967 and 2.065 Å, respectively. In **6**, the bmb adopt two kinds of conformations. One takes *trans*-conformation with a $N_{donor}\cdots N-C_{sp3}\cdots C_{sp3}$ torsion angle of 76.360°, which bridges two adjacent Zn^{II} ions with a Zn···Zn distance of 14.091 Å. The other shows a twisted *cis*-conformation with the dihedral angles between the pairs of benzimidazole rings being 48.611° in contrast to those in above complexes being 180°. The $N_{donor}\cdots N-C_{sp3}\cdots C_{sp3}$ torsion angle (44.422°) of *cis*-conformational bmb is the smallest in complexes **1**−**7**. The *cis*-conformational bmb exhibits a "V" shape

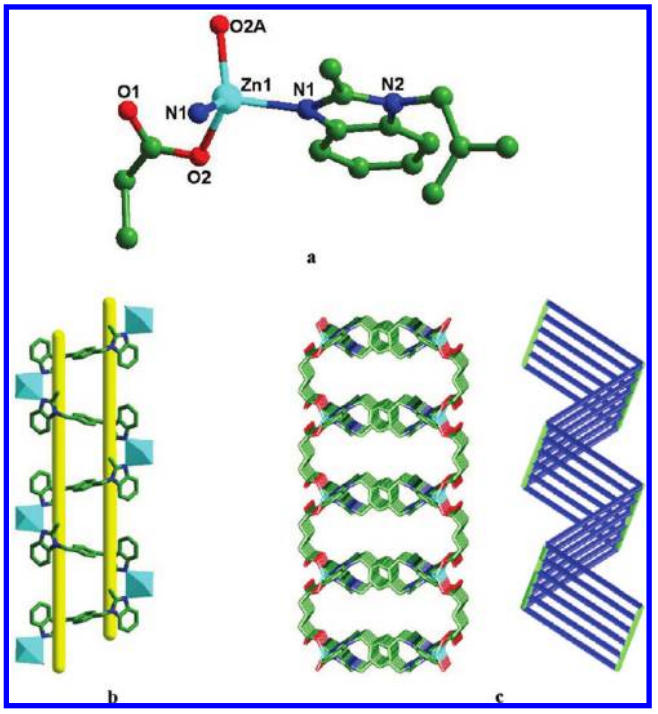

Figure 7. (a) Coordination environment of Zn^{II} ion in **7** with hydrogen atoms and free water molecules omitted for clarity. (b) The bmb ligands adopt a *trans*-conformation and link the adjoining Zn^{II} ions into a 1D meso-helical chain. (c) The adjacent Zn^{II}-bmb meso-helical chains are connected by long glu^{2-} anions to give a 2D puckered (4, 4) network with striplike channels.

to coordinate with two adjacent Zn^{II} ions, and the Zn···Zn separation is 10.4232 Å, which is obviously shorter than that of *trans*-conformational bmb. The *cis*- and *trans*-conformational bmb are linked by Zn^{II} ions alternately to form an infrequent single-strand interweaved meso-helix (Figure 6b) with a long helical pitch of 21.025(4) Å corresponding to the length of *c*-axis. Surprisingly, a further study reveals that the configuration of the single-strand interweaved meso-helix shows a unique feature with one helix consisting of four flexures in one single strand, which can be suggested as "tetra-flexural helix".[15] All of the points of flexure on the edge of the spiral line are Zn^{II} ions. The most puzzling feature is that each meso-helical chain entangles four spiral shafts. The four shafts are entwined as the sequence b−c−a−d (Figure 6b). Viewing from the *c*-axis, the projection of the helical chain on the *ab* plane looks like a pair of swallows standing face to face (Figure 6c). To our knowledge, there is only one known example of tetra-flexural helix,[15] and our research further enriches the isomers chemistry related to the helices.

On the other hand, the suc^{2-} anions with bimonodentate mode bridge adjacent Zn^{II} ions to form a left-hand helix. The helical pitch is 10.8870 Å corresponding to the length of *b*-axis (Figure 6d). The Zn^{II}-suc left-hand helix and Zn^{II}-bmb tetra-flexural helix construct a 3D framework with 6^6 topology (Figure 6e) by sharing Zn^{II} ions.

Crystal Structure of $\{[Zn(bmb)(glu)]\cdot H_2O\}_n$ (**7**). The Zn^{II} ion is four-coordinated by two carboxylic oxygen atoms (O2, O2A) from two glu^{2-} anions and two nitrogen atoms (N1, N1A) from two bmb in a distorted tetrahedral environment (ZnO_2N_2) (Figure 7a). The Zn−O and Zn−N bond lengths are 1.933(5) and 2.072(5) Å, respectively, falling into the normal range.[13] The glu^{2-} shows a *cis*-conformation with two carboxylic groups bending in the same direction, which adopts bimonodentate mode to bridge adjacent Zn^{II} ions with a Zn···Zn distance of 8.668 Å. The bmb exhibits *trans*-conformation with a $N_{donor}\cdots N-C_{sp3}\cdots C_{sp3}$ torsion angle of 85.898°. The pair of benzimidazole rings bending in the opposite direction bridge adjacent Zn^{II} ions to give a "∞" shape meso-helical chain (Figure 7b). The Zn···Zn distance across bmb is 12.7819 Å, and the helical pitch is 15.938 Å corresponding to the length of *b*-axis. As shown in Figure 7c, the adjacent Zn-bmb meso-helical chains are further connected by long glu^{2-} anions as pillars to give a 2D puckered (4, 4) network with striplike channels.

XRD Patterns and Thermal Analyses. To confirm the phase purity of these complexes, the PXRD patterns were recorded for complexes **1**−**7**, and they were comparable to the corresponding simulated ones calculated from the single-crystal diffraction data (Figure S1 in the Supporting Information), indicating a pure phase of each bulky sample.

The thermal stability of the seven complexes was also estimated (Figure S2 in the Supporting Information). Complex **1** shows a weight loss of 2.90% from 30 to 115 °C corresponding to the release of lattice water molecule (calcd, 2.85%), and then, a plateau region is observed. The coordinated water molecule and uncoordinated ligand bmb, together with overall framework begin to decompose from 282 °C, which probably results from the presence of hydrogen bonding between the coordinated water molecules and the uncoordinated ligand bmb.[16] For complex **2**, a weight loss of 5.60% is detected in the range of 70−140 °C corresponding to the loss of two lattice water molecules (calcd, 5.69%), and then, a plateau region follows. The further weight loss is observed at about 313 °C due to the decomposition of overall framework. No obvious weight loss is observed for anhydrous complex **3** until the decomposition of the framework occurs at 380 °C. For complex **4**, a slow weight loss of 3.68% occurs before 378 °C corresponding to the loss of coordinated water (calcd, 4.18%), and then, the framework begins to collapse. The unusual slow weight loss of coordinated water may be because the hydrogen-bonding interactions. For anhydrous complex **5**, a weight loss of 3.47% appears in the range of 30−150 °C, which is probably attributed to the adsorptive water molecules from the air. Then, the framework collapses at 351 °C. Complex **6** loses 4.98% of weight in the range of 30−130 °C, which is attributed to the departure of three lattice water molecules (calcd, 4.70%), and the framework is stable up to 311 °C. In complex **7**, a weight loss of the lattice water molecule (3.50%) occurs in the range of 30−126 °C (calcd, 3.11%). The main framework remains intact until it is heated to 304 °C.

Photoluminescence Properties. Coordination polymers with d^{10} metal centers and conjugated organic linkers are promising candidates for photoactive materials with potential applications such as chemical sensors and photochemistry.[17] Hence, the solid state photoluminescence properties of Zn^{II} complexes **1**−**7**, together with the free bmb ligand and all of the dicarboxylic acids were investigated at room temperature (Figure S3 in the Supporting Information). Under the same experimental conditions, the emission intensities of 2,6-H_2pydc, H_2fum, H_2suc, and H_2glu are much weaker than that of N-donor ligand bmb, so it is considered that they have no significant contribution to the fluorescent emission of the complexes with the presence of bmb. The free ligands bmb, o-H_2bdc, m-H_2bdc, and p-H_2bdc show intense emissions bands at 309 nm (λ_{ex} = 293 nm), 343 nm (λ_{ex} = 306 nm), 360 nm (λ_{ex} = 310 nm), and 383 nm (λ_{ex} = 314 nm),

respectively. Obviously, the fluorescent emissions bands of **1** (λ_{em} = 308 nm, λ_{ex} = 280 nm), **3** (λ_{em} = 304 nm, λ_{ex} = 270 nm), **5** (λ_{em} = 301 nm, λ_{ex} = 282 nm), and **6** (λ_{em} = 303 nm, λ_{ex} = 285 nm) can be attributed to the intraligand charge transitions of bmb due to their similar emission bands. Notably, large red-shifted emission occurs in **2** (λ_{em} = 441 nm, λ_{ex} = 360 nm), and such broad band may be tentatively assigned to ligand-to-metal charge transfer (LMCT) as reported for other Zn^{II} complexes with N-donor ligands.[18] As to **4**, the emission of 351 nm (λ_{ex} = 290 nm) with a small red-shifted is probably caused by the coordination of bmb to the metal centers, and the emission of 482 nm (λ_{ex} = 337 nm) with a large red-shifted as compared with the ligand p-H_2bdc may be tentatively assigned to LMCT.[19] Complex **7** exhibits two emission bands at 303 and 408 nm (λ_{ex} = 280 nm), respectively. The emission of 303 nm can be attributed to the intraligand charge transitions of bmb, and the emission of 408 nm may be assigned to LMCT. In addition, further investigation indicates that the fluorescent intensities of complexes **1**−**7** dramatically decrease as compared with the corresponding ligands. It may be attributed to the helical features in complex **1**−**7**, which lower the rigidity of the ligands and increase the loss of energy via vibration motions. The results indicate that the structures of complexes have subtle but significant influences on the photoluminescent intensities.

CONCLUSIONS

In summary, by introducing a series of dicarboxylate organic molecules with different spacer angles and lengths as coligands, novel Zn^{II}-bmb meso-helical complexes have been successfully constructed. The results show that the use of semirigid ligand bmb is a feasible route to synthesize and formulate meso-helical structures. In addition, the dicarboxylate coligands can effectively tune of the meso-helical features and build much more complicated and fascinating MOFs. Our present findings offer the possibility of controlling the formation of desired meso-helical characters and further enrich the crystal engineering strategy. Moreover, the investigation of photoluminescence properties indicates that the formation of helix can weaken the fluorescent intensities of MOFs.

ASSOCIATED CONTENT

Supporting Information. X-ray crystallographic files in CIF format, selected bond lengths and bond angles, powder X-ray patterns, TGA curves, photoluminescences for **1**−**7**, and the structural formulas of the ligands. This material is available free of charge via the Internet at http://pubs.acs.org.

AUTHOR INFORMATION

Corresponding Author

*Fax: (86)0371-67761744. E-mail: houhongw@zzu.edu.cn.

ACKNOWLEDGMENT

This work was financially supported by the National Natural Science Foundation (Nos. 20971110 and 91022013), Program for New Century Excellent Talents of Ministry of Education of China (NCET-07-0765), the Outstanding Talented Persons Foundation of Henan Province, and The Ministry of Science and Technology of China for the International Science Linkages Program (2009DFA50620).

REFERENCES

(1) (a) Klug, A. *Angew. Chem., Int. Ed.* **1983**, *22*, 565. (b) Orr, G. W.; Barbour, L. J.; Atwood, J. L. *Science* **1999**, *285*, 1049. (c) Bu, X.-H.; Tong, M.-L.; Chang, H.-C.; Kitagawa, S.; Batten, S. R. *Angew. Chem., Int. Ed.* **2004**, *43*, 192. (d) Zhang, J.-P.; Lin, Y.-Y.; Huang, X.-C.; Chen, X.-M. *Chem. Commun.* **2005**, 1258. (e) Ye, B. H.; Tong, M. L.; Chen, X. M. *Coord. Chem. Rev.* **2005**, *249*, 545. (f) Zhao, J.; Mi, L.; Hu, J.; Hou, H.; Fan, Y. *J. Am. Chem. Soc.* **2008**, *130*, 15222. (g) Lu, T.-B.; Zheng, X.-D. *CrystEngComm* **2010**, *12*, 324. (h) Ramaswamy, A.; Froeyen, M.; Herdewijn, P.; Ceulemans, A. *J. Am. Chem. Soc.* **2010**, *132*, 587.

(2) (a) Berl, V.; Huc, I.; Khoury, R. G.; Krische, M. J.; Lehn, J. M. *Nature* **2000**, *407*, 720. (b) Hannon, M. J.; Moreno, V.; Prieto, M. J.; Moldrheim, E.; Sletten, E.; Meistermann, I.; Isaac, C. J.; Sanders, K. J.; Rodger, A. *Angew. Chem., Int. Ed.* **2001**, *40*, 880. (c) Tabellion, F. M.; Seidel, S. R.; Arif, A. M.; Stang, P. J. *J. Am. Chem. Soc.* **2001**, *123*, 7740. (d) Malabika, N.; Rajesh, K.; Helen, S. E.; Sasankasekhar, M. *Cryst. Growth Des.* **2005**, *5*, 1907. (e) Suen, M.-C.; Chan, Z.-K.; Chen, J.-D.; Wang, J.-C.; Hung, C.-H. *Polyhedron* **2006**, *25*, 2325. (f) Li, S.-L.; Lan, Y.-Q.; Qin, J.-S.; Ma, J.-F.; Liu, J.; Yang, J. *Cryst. Growth Des.* **2009**, *9*, 4142. (g) Zhang, G.; Yao, S.-Y.; Guo, D.-W.; Tian, Y. Q. *Cryst. Growth Des.* **2010**, *10*, 2355. (h) Yang, G.-P.; Liu, B.; Hou, L.; Liu, P.; Liu, B.; Wang, Y.-Y.; Shi, Q.-Z. *Inorg. Chem. Commun.* **2011**, DOI: 10.1016/j.inoche.2011.01.020.

(3) (a) Becker, G.; Eschbach, B.; Mundt, O.; Seidler, N. *Z. Anorg. Allg. Chem.* **1994**, *620*, 1381. (b) Plasseraud, L.; Maid, H.; Hampel, F.; Saalfrank, R. W. *Chem.—Eur. J.* **2001**, *7*, 4007. (c) Xiao, D. R.; Li, Y. G.; Wang, E. B.; Fan, L. L.; An, H. Y.; Su, Z. M.; Xu, L. *Inorg. Chem.* **2007**, *46*, 4158. (d) Qi, Y.; Luo, F.; Batten, S. R.; Che, Y. X.; Zheng, J. M. *Cryst. Growth Des.* **2008**, *8*, 2806. (e) Jin, J.-C.; Wang, Y.-Y.; Liu, P.; Liu, R.-T.; Ren, C.; Shi, Q.-Z. *Cryst. Growth Des.* **2010**, *10*, 2029.

(4) (a) Xiao, A.-R.; Li, Y.-G.; Wang, E.-B.; Fan, L.-L.; An, H.-Y.; Su, Z.-M.; Xu, Lin. *Inorg. Chem.* **2007**, *46*, 4158. (b) Ashiry, K. O.; Zhao, Y.-H.; Shao, K.-Z.; Su, Z.-M.; Fu, Y.-M.; Hao, X.-R. *Inorg. Chem. Commun.* **2008**, *11*, 1181. (c) Chen, J.-Q.; Cai, Y.-P.; Fang, H.-C.; Zhou, Z.-Y.; Zhan, X.-L.; Zhao, G.; Zhang, Z. *Cryst. Growth Des.* **2009**, *9*, 1605.

(5) (a) Du, J.-L.; Hu, T.-L.; Zhang, S.-; Zeng, Y.-F.; Bu, X.-H. *CrystEngComm* **2008**, *10*, 1866. (b) Qiu, Y.; Deng, H.; Yang, S.; Mou, J.; Daiguebonne, C.; Kerbellec, N.; Guillou, O.; Batten, S. R. *Inorg. Chem.* **2009**, *48*, 4158. (c) Zhang, Q.; He, L.; Liu, J.-M.; Wang, W.; Zhang, J.; Su, C.-Y. *Dalton Trans.* **2010**, *39*, 11171. (d) Sumida, K.; Foo, M. L.; Horike, S.; Long, J. R. *Eur. J. Inorg. Chem.* **2010**, 3739.

(6) (a) Ok, K. M.; O'Hare, D. *Dalton Trans.* **2008**, 5560. (b) Perry, J. J., IV; Perman, J. A.; Zaworotko, M. J. *Chem. Soc. Rev.* **2009**, *38*, 1400. (c) Ma, S.; Simmons, J. M.; Yuan, D.; Li, J.-R.; Weng, W.; Liua, D.-J.; Zhou, H.-C. *Chem. Commun.* **2009**, 4049. (d) Liu, J.-Q.; Liu, B.; Wang, Y.-Y.; Liu, P.; Yang, G.-P.; Liu, R.-T.; Shi, Q.-Z.; Batten, S. R. *Inorg. Chem.* **2010**, *49*, 3739. (e) Qiu, W.; Perman, J. A.; Wojtas, Ł.; Eddaoudia, M.; Zaworotko, M. J. *Chem. Commun.* **2010**, *46*, 8734.

(7) (a) Ye, B.-H.; Ding, B.-B.; Weng, Y.-Q.; Chen, X.-M. *Cryst. Growth Des.* **2005**, *5*, 801. (b) Dv̈ren, T.; Baeb, Y.-S.; Snurr, R. Q. *Chem. Soc. Rev.* **2009**, *38*, 1237. (c) Li, J.-R.; Yakovenko, A. A.; Lu, W.; Timmons, D. J.; Zhuang, W.; Yuan, D.; Zhou, H.-C. *J. Am. Chem. Soc.* **2010**, *132*, 17599. (d) Blake, K. M.; Johnston, L. L.; Nettleman, J. H.; Supkowski, R. M.; LaDuca, R. L. *CrystEngComm* **2010**, *12*, 1927.

(8) (a) Li, J.-R.; Timmons, D. J.; Zhou, H.-C. *J. Am. Chem. Soc.* **2009**, *131*, 6368. (b) Zheng, S.; Wu, T.; Zhang, J.; Chow, M.; Nieto, R.; A. Feng, P.; Bu, X. *Angew. Chem., Int. Ed.* **2010**, *49*, 1. (c) Yang, J.; Li, B.; Ma, J.-F.; Liu, Y.-Y.; Zhang, J.-P. *Chem. Commun.* **2010**, *46*, 8383. (d) Xu, Y.; Chen, P.-K.; Che, Y.-X.; Zheng, J.-M. *Eur. J. Inorg. Chem.* **2010**, 5478.

(9) Aakeroÿ, C. B.; Desper, J.; Leonard, B.; Urbina, J. F. *Cryst. Growth Des.* **2005**, *5*, 865.

(10) Sheldrick, G. M. *Acta Crystallogr.* **2008**, *A64*, 112.

(11) (a) Meng, X.; Song, Y.; Hou, H.; Han, H.; Xiao, B.; Fan, Y.; Zhu, Y. *Inorg. Chem.* **2004**, *43*, 5478. (b) Zhang, Q.; Zhang, J.; Yu, Q.-Y.; Pan, M.; Su, C.-Y. *Cryst. Growth Des.* **2010**, *10*, 4076.

(12) Yang, G.-P.; Wang, Y.-Y.; Liu, P.; Fu, A.-Y.; Zhang, Y.-N.; Jin, J.-C.; Shi, Q.-Z. *Cryst. Growth Des.* **2010**, *10*, 1443.

(13) (a) Li, X.; Gao, R.; Sun, D.; Bi, W.; Wang, Y.; Li, X.; Hong, M. *Cryst. Growth Des.* **2004**, *4*, 775. (b) Braverman, M. A.; LaDuca, R. L. *Cryst. Growth Des.* **2007**, *7*, 2343.

(14) (a) Suh, M. P.; Choi, H. J.; So, S. M.; Kim, B. M. *Inorg. Chem.* **2003**, *42*, 676. (b) Zhang, X.-L.; Guo, C.-P.; Yang, Q.-Y.; Wang, W.; Liu, W.-S.; Kanga, B.-S.; Su, C.-Y. *Chem. Commun.* **2007**, 4242. (c) Byrne, P.; Lloyd, G. O.; Clarke, N.; Steed, J. W. *Angew. Chem., Int. Ed.* **2008**, *47*, 5761.

(15) Dong, Z.; Wang, Y.-Y.; Liu, R.-T.; Liu, J.-Q.; Cui, L.; Shi, Q.-Z. *Cryst. Growth Des.* **2010**, *10*, 3311.

(16) Zhang, W.-L.; Liu, Y.-Y.; Ma, J.-F.; Jiang, H.; Yang, Jin.; Ping, G.-J. *Cryst. Growth Des.* **2008**, *8*, 1250.

(17) (a) Yue, C.; Yan, C.; Feng, R.; Wu, M.; Chen, L.; Jiang, F.; Hong, M. *Inorg. Chem.* **2009**, *48*, 2873. (b) Allendorf, M. D.; Bauer, C. A.; Bhaktaa, R. K.; Houka, R. J. T. *Chem. Soc. Rev.* **2009**, *38*, 1330. (c) Hu, J.; Zhao, J.; Guo, Q.; Hou, H.; Fan, Y. *Inorg. Chem.* **2010**, *49*, 3679. (d) Yao, X.-Q.; Cao, D.-P.; Hu, J.-S.; Li, Y.-Z.; Guo, Z.-J.; Zheng, H.-G. *Cryst. Growth Des.* **2011**, *11*, 231.

(18) Liu, H.-Y.; Wu, H.; Ma, J.-F.; Liu, Y.-Y.; Liu, B.; Yang, J. *Cryst. Growth Des.* **2010**, *11*, 4795.

(19) Zheng, S.-L.; Yang, J.-H.; Yu, X.-L.; Chen, X.-M.; Wong, W.-T. *Inorg. Chem.* **2004**, *43*, 830.